LIMNOLOGY AND OCEANOGRAPHY
Letters

ASLO
Open Access

Limnology and Oceanography Letters 6, 2021, 320–328

doi: 10.1002/lol2.10209

LETTER

Microbial methane oxidation efficiency and robustness during lake overturn

M. Zimmermann [1,2] *M. J. Mayr* [1,2] *H. Bürgmann* [1]* *W. Eugster* [2] *T. Steinsberger* [1] *B. Wehrli* [1,2] *A. Brand* [1a] *D. Bouffard* [1]

[1]Eawag, Swiss Federal Institute of Aquatic Science and Technology, Surface Waters - Research and Management, Kastanienbaum, Switzerland; [2]Departement of Environmental Systems Science, ETH Zürich, Zürich, Switzerland

Scientific Significance Statement

Methane is emitted from lakes in globally significant amounts. In temperate stratified lakes, substantial amounts of dissolved methane can accumulate in the hypolimnion and reach the surface through vertical mixing during lake overturn. The effectiveness of methanotrophic bacteria in oxidizing methane before it can escape to the atmosphere is an ongoing controversy. With this study, we identify the key processes that control the efficiency and robustness of the microbial methane conversion process. We present evidence for efficient and robust methane oxidation under a large range of mixing regimes in a seasonally stratified lake. In the context of climate change, our results suggest that changes in the frequency of exceptional storm events may be more important for methane emissions from temperate lakes than gradual warming.

Abstract

Many seasonally stratified lakes accumulate substantial amounts of the greenhouse gas methane in the anoxic zone. Methane oxidizing bacteria in the water column act as a converter, oxidizing methane into carbon dioxide and biomass before it reaches the atmosphere. Current observations and estimates of this methane oxidation efficiency are diverging, especially for the lake overturn period. Here, we combine a model of turbulent mixing, gas exchange, and microbial growth with a comprehensive data set for autumn mixing to quantify the relevant physical and microbial processes for a 16 m deep, wind-sheltered Swiss lake. Scenario analysis suggests that the methane converter is efficient and robust under a large range of mixing velocities and only rare events

*Correspondence: helmut.buergmann@eawag.ch

[a]Present address: Furkastrasse 75, 3904 Naters, Switzerland

Associate editor: John Anderson

Author Contribution Statement: MZ, MJM, AB, and HB conceptualized the research program and field campaigns. MZ and DB conceptualized the box model approach. MZ and MJM carried out the field campaigns, TS took and analyzed the sediment samples and WE performed eddy flux measurements. MZ and MJM curated, analyzed, and visualized the data from the field campaigns; MZ performed and visualized the model simulations. MZ wrote the original draft of the manuscript with contributions from MJM, DB, BW, HB, and WE. HB and AB acquired the funding.

Data Availability Statement: Data and metadata used for this publication are available on the ETH Research Collection (https://doi.org/10.3929/ethz-b-000350091). Meteorological data were obtained from MeteoSwiss (www.meteoswiss.admin.ch). The source code of the generic model is available as a Julia package on GitHub: https://github.com/zimmermm/ConvectionBoxmodel.jl. The actual implementation for Lake Rotsee is attached to the data package on the ETH Research Collection (https://doi.org/10.3929/ethz-b-000350091).

Additional Supporting Information may be found in the online version of this article.

of pronounced surface cooling can trigger substantial outgassing. This case study combines in situ observation and a deterministic physically based model and suggests that the frequency of storms may strongly impact methane emissions for similar temperate lakes.

Lakes and reservoirs are increasingly recognized as significant players in the global carbon cycle because they store, convert, and release substantial amounts of greenhouse gases (Tranvik et al. 2018). According to recent estimates, lacustrine methane emissions are responsible for about 75% of the climate impact of lacustrine systems (DelSontro et al. 2018) showing an increasing trend (Beaulieu et al. 2019). In lakes, most methane is produced in the anaerobic sediment (Bastviken et al. 2008) and ultimately either released to the atmosphere or oxidized by aerobic methane oxidizing bacteria (MOB), which use methane as their sole carbon and energy source (Hanson and Hanson 1996). In addition to the diffusive transport of methane to the atmosphere, ebullition of methane is an important pathway and responsible for the majority of methane emissions in certain systems (DelSontro et al. 2011; Schmid et al. 2017). Here, we focus on the fate of dissolved methane during lake overturn and provide evidence that this microbial methane converter is efficient and robust even at high rates of vertical mixing thereby preventing a major fraction of dissolved methane from outgassing.

This microbial methane sink has important implications for lakes with seasonal thermal stratification that accumulate large amounts of dissolved methane in the anoxic hypolimnion, hereafter referred to as "stored methane." During stratification, MOB at the oxic–anoxic interface form an effective barrier against diffusive methane outgassing, which is only bypassed by ebullition, that is, methane bubbles released from the sediment (DelSontro et al. 2011). In contrast, strong vertical mixing during the autumn overturn may lead to a rapid transport of stored methane to the surface. So far, estimates of global methane emissions from lakes have therefore assumed that most of this stored methane is ultimately released to the atmosphere (Bastviken et al. 2004). However, the supply of methane to the oxygen-rich surface water creates favorable conditions for the growth of aerobic MOB (Mayr et al. 2020*a*). If the MOB community grows fast enough, it could significantly reduce the emission of stored methane even during lake overturn.

Published field measurements of the percentage of stored methane that is oxidized range from 54% to 94% (Utsumi et al. 1998; Kankaala et al. 2007; Schubert et al. 2012; Encinas Fernández et al. 2014). These studies focused either on time-resolved flux measurements (Utsumi et al. 1998; Bastviken et al. 2004) or on microbial rate observations (Kankaala et al. 2007; Schubert et al. 2012). Here, we closely integrate the two approaches in a comprehensive field campaign on Rotsee, a small, 16-m deep, wind-sheltered lake located in central Switzerland, in order to improve our understanding of the underlying processes during lake overturn. Compared to quasi steady-state models for methane oxidation (Thottathil et al. 2019), we focus our effort on the dynamics of the lake turnover with its high potential for methane release.

Based on data from the field campaign, we developed and validated a dynamic model of turbulent mixing, methane transport, gas exchange, and Monod-type MOB growth. We then quantified the efficiency of the methane converter and tested the robustness of this efficiency for different wind and convective mixing regimes during the autumn overturn.

Methods

Field measurements

We determined the fate (storage, emission into the atmosphere, microbial oxidation) of methane stored in the hypolimnion during seven field campaigns over the course of the autumn overturn from October to December 2016 in Lake Rotsee, Switzerland. Study site details and measurement methods are given in the Supporting Information. We recorded the state of stratification by measurements of water temperature with a temporal resolution of 5 s and a spatial resolution of 1 m (RBRconcerto T24 thermistor string, RBR). We measured methane concentrations in the water column and in two duplicate sediment cores using the headspace equilibration method by gas chromatography (Agilent 6890N, USA). We determined MOB cell numbers using catalyzed reporter deposition fluorescence in situ hybridization (CARD-FISH) and epifluorescence microscopy and converted the cell numbers to biomass using an average cellular carbon content of 0.42 pg cell^{-1} based on literature values (Posch et al. 2001; Romanova and Sazhin 2010; Oswald et al. 2015). We quantified methane emissions with eddy-covariance flux measurements as described in Sollberger et al. (2017) and Eugster and Plüss (2010).

Methane budget

We calculated the methane budget neglecting potential horizontal variability. Total amounts of methane and biomass in the water column were calculated as volume integrated mass of carbon. Methane emissions were extrapolated to the whole lake surface area and are given as cumulative amounts of carbon. We used the standard deviation (SD) when the variability was of interest and the standard error of the mean (SEM) or the 95% confidence interval (CI) when the uncertainty of the mean was of interest. The error values provided

in the results section are based on the standard deviation, unless explicitly stated differently. Confidence intervals were corrected for sample size using the *t* statistic.

Mechanistic model

We used a set of differential equations, describing the most relevant physical, chemical, and biological processes, to investigate the efficiency and robustness of microbial methane oxidation during lake overturn. We approximated the mixed layer as a single, homogeneously mixed box, which gets larger as the thermocline deepens. The system of ordinary differential equations describing the temporal evolution of the mixed layer depth, temperature, methane concentration, and MOB biomass is described in the Supporting Information. We parameterized the deepening of the mixed layer as a function of convective and wind-driven forcing (Driedonks 1982; Batchvarova and Gryning 1991). We calculated the flux of methane into the mixed box based on the simulated speed of thermocline deepening and the profile of maximum methane concentration in the hypolimnion (Supplementary Fig. S2). We calculated methane emissions with the boundary layer model of Liss and Slater (1974) that has already been successfully used for Lake Rotsee (Schubert et al. 2012) and we applied the surface-renewal model (Lorke and Peeters 2006) to account for the contribution of wind and convection to the transfer velocities. In the mixed layer, we assumed that methane is the limiting nutrient and we formulate the growth rate of MOB with a Monod-type methane oxidation kinetics, the most commonly used growth model for suspended microbial cells (Kovárová-Kovar and Egli 1998). We use the carbon conversion efficiency (CCE) to determine how much of the oxidized methane contributes to growth of MOB biomass. We obtained the kinetic parameters by calibration with the measured biomass development (Supplementary Table S1).

The biogeochemical model starts with initial temperature and methane profiles and uses meteorological data (wind speed, air-temperature, incoming longwave radiation, global radiation, and humidity) to calculate the deepening of the thermocline and the exchange of methane with the atmosphere.

Scenario analysis

Because Lake Rotsee is wind-sheltered, we explored the effect of various wind regimes on methane emissions by a model scenario analysis. We set wind speeds to a constant level for 12 h or 3 d. Each scenario consisted of a single wind-event that started at a specified mixed-layer depth. To avoid artifacts from other meteorological conditions during the wind-event, we neglected the heat balance during this period and calculated the forced convection based on an empirical regression between the friction velocity and the buoyancy flux at the surface (Supplementary Fig. S4).

Results and discussion

Fate of methane during the autumn overturn

We determined the fate of methane in a small temperate lake during the autumn overturn (Fig. 1). From October to December 2016, only 9% of the stored methane that was transported to the surface was emitted to the atmosphere. Methane emissions determined by eddy covariance flux measurement were on average 0.26 μg CH_4 m^{-2} s^{-1} and summed to a total of 0.36 Mg C for the whole lake (Fig. 1a). During this period, cooling of the surface water as well as wind (Fig. 1a) increased the mixed-layer depth from 7.6 to 13 m (Fig. 1b). This physical process gradually depleted the methane pool in the hypolimnion and transferred a total of 4.2 Mg C of methane to the mixed layer. After subtraction of the emissions, the remaining 3.8 Mg C either were oxidized by MOB or remained in the mixed layer. However, we only measured mixed layer methane concentrations of 0.5 ± 0.4 μM or a maximum total methane inventory of 0.039 ± 0.026 Mg C, suggesting that MOB oxidized about 91% of the stored methane. In parallel, MOB cell numbers in the mixed layer increased from ~2×10^4 cell mL^{-1} to 3×10^5 cell mL^{-1} (Fig. 1c), which corresponds to a cumulative biomass increase by a factor of factor 14, from 0.047 to 0.67 Mg C. Despite this rapid growth, the 0.62 Mg C of newly formed biomass represented a small fraction of the 3.8 Mg C that were supplied to the mixed layer, suggesting a net CCE of MOB of only 0.16. The calculated biomasses are a conservative estimate because we neglect grazing (Devlin et al. 2015). An additional uncertainty of about 40% comes from the range of reported cellular carbon contents (0.26–0.57 pg $cell^{-1}$). We limit the effect of uncertain biomass estimates by calibrating the CCE in the model, where our emission measurements serve as an additional boundary condition. With the increase of MOB biomass, we observed a change not only in the community composition but also in the dominant kinetic traits of the MOB assemblage (Mayr et al. 2020*a*,*b*).

Modeling the key processes

Based on these field observations, we validated a numerical model of the key processes (Fig. 2) that determine the fate of stored methane and control the efficiency and robustness of the microbial methane converter during the autumn overturn. Despite its simplicity, the turbulent mixing model reproduced the evolution of the measured mixed-layer depth (Fig. 2a) with a root mean square error (RMSE) of only 0.27 m. The modeled flux of stored methane to the mixed layer was in good agreement with the measurements (Fig. 2b). The Monod-type growth model reproduced the evolution of MOB biomass to a maximum of 0.68 Mg C with a RMSE of 0.061 Mg C (Fig. 2c). The consideration of microbial growth makes a substantial difference to models that assume a first order rate constant because the growing microbial biomass results in an increasing methane oxidation rate. Recent studies showed that MOB abundance and methane oxidation rates

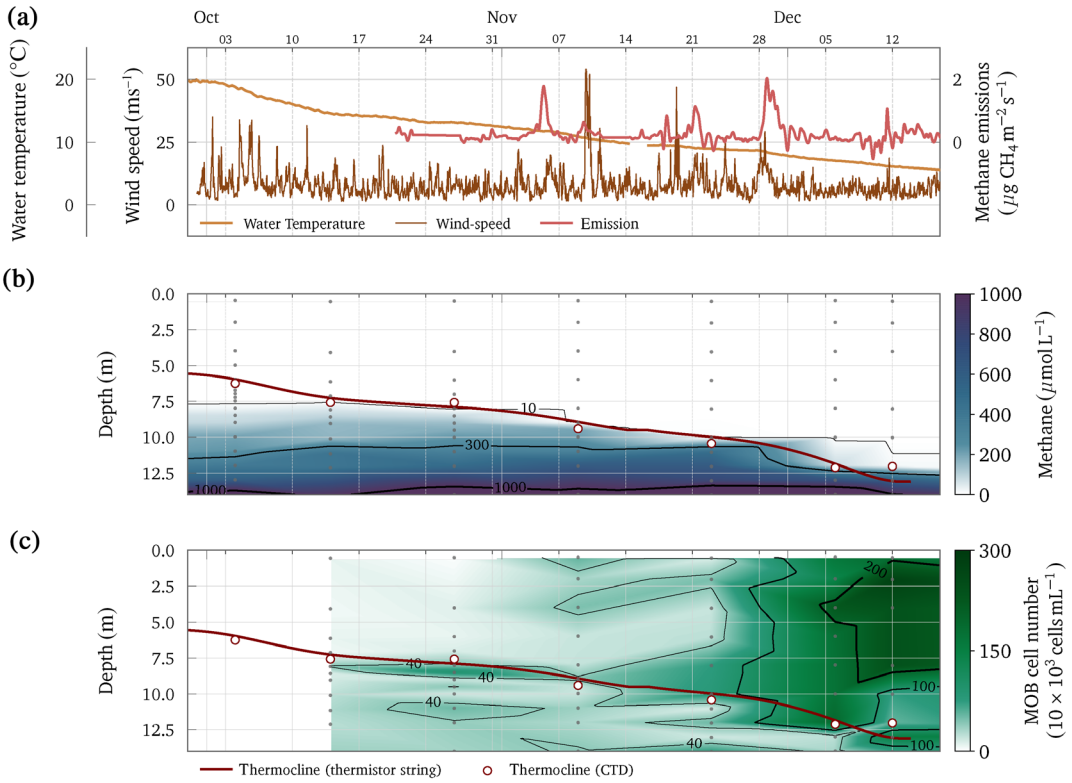

Fig 1. Field observations during the overturn period 2016 in Lake Rotsee. The horizontal time axis for all panels is plotted on top. Major ticks indicate the start of the month and minor ticks refer to the dates. (**a**) The daily average surface water temperature is plotted as a proxy for the progressing cooling during the overturn period. Wind speeds from the closest automated weather station (www.meteoswiss.ch) are plotted as hourly averages and were corrected for Lake Rotsee (Supplementary Fig. S1). Methane emissions are plotted as Gaussian filtered flux of the measured 30 min average fluxes. (**b**) Methane concentrations in the water column are plotted as a heatmap interpolated from individual measurements that are indicated by gray dots. Methane concentrations in the mixed layer were 0.5 ± 0.4 μM but reached up to 3.7 mM at the sediment–water interface (Supplementary Fig. S2), which corresponds to a partial pressure of about 65% at this depth. The depth of the thermocline was interpolated from the continuous thermistor string data and was verified by individual CTD profiles. (**c**) Cell numbers of MOB are plotted as a heatmap interpolated from individual measurements that are indicated by gray dots. On 12 December, the low cell number at 10 m might be a measurement error because the temperature profiles indicate complete mixing to 12.5 m.

negatively correlated with oxygen concentration during the stratified period (Thottathil et al. 2019; Reis et al. 2020). The expected impact of oxygen-inhibition remains poorly constrained and may in addition vary among different MOB assemblages, which were highly dynamic during the mixing period (Mayr et al. 2020*a*). Oxygen concentrations in the mixed layer varied in a limited range (175–412 μM; Mayr et al. 2020*a*) compared to the gradients of stratified lakes where this phenomenon has been observed and were always several orders of magnitude higher than methane (<0.05–1.1 μM), so oxygen limitation is likewise not relevant. Any inhibition is therefore probably relatively constant and integrated into the fitted parameters. In the context of this study, we therefore refrained from explicitly implementing oxygen inhibition in the model. The good fit of the model supports the validity of the approach.

The box model approach also neglected a potential gradual crossover of methane and oxygen within the thermocline. However, the biomass profiles did not give any indication that such a transition zone was of particular importance for methane oxidation during the overturn period (Fig. 1c).

The ratio of modeled methane emission to the total transport of stored methane to the mixed layer suggests that about 98% of this methane was oxidized by MOB. The measured cumulative methane flux to the atmosphere was about three times larger than the modeled flux (Fig. 2d). Since the model only accounts for atmospheric emissions from diffusive flux, this discrepancy likely stems from the contribution of methane ebullition to the emissions during the overturn. That ebullition is a major pathway during the autumn overturn in Lake Rotsee was shown in a study by Schubert et al. (2012) who estimated cumulative contributions of ebullition to total emissions between 88% and 97%. A similar study (Vachon et al. 2019) in a nearby, similarly small wind-sheltered lake (Soppensee located 17 km from Rotsee) reported a mean sediment ebullition rate of 1.4 mmol m^{-2} d^{-1}. Taking this value

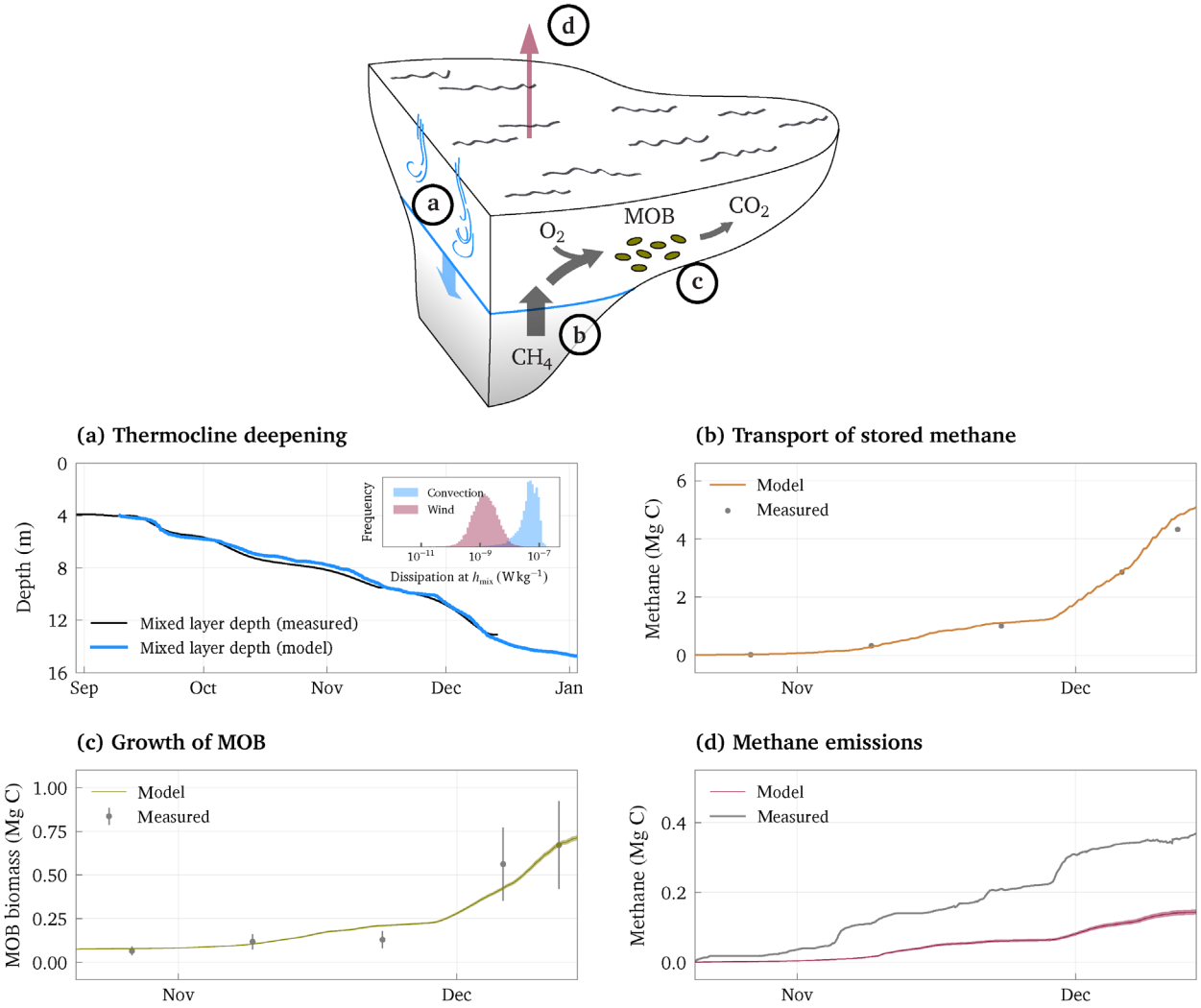

Fig 2. Model combining the key processes that determine the fate of stored methane during the autumn overturn. (**a**) The deepening of the thermocline was modeled using a turbulent mixing model that considers wind-driven and thermal convection. Modeled and measured depth of the thermocline fit very well. The inset shows the histogram of the dissipation rate of convective and wind-driven turbulent kinetic energy at the mixed-layer depth over the simulation period. (**b**) Modeled and measured cumulative amount of stored methane transported to the mixed layer. (**c**) Modeled and measured MOB biomass. The error bars for the measured biomasses represent 95% confidence intervals for the biomass, based on the uncertainty in the cellular carbon content. (**d**) Modeled and measured cumulative emissions of methane to the atmosphere. Emissions measured by eddy covariance also include ebullition, whereas the model does not include this emission pathway.

and assuming 30% re-dissolution (Vachon et al. 2019) over the mean lake depth for Rotsee, that is, 8.7 m, we obtained a cumulative methane emission via ebullition over the studied period of ~ 0.2 Mg C and a total emission of 0.37 Mg C which is remarkably close to the observations (Fig. 2d).

Even though the model does not take into account the observed diversity of the MOB community (Mayr et al. 2020*a*), the fitted bulk kinetic parameter are comparable with expected properties for the methane-limiting conditions in the mixed layer. The half saturation constant for methane oxidation (K_{M,CH_4}) of 1.7 μM is in the lower range of published values (1 and 10 μM) (Hanson and Hanson 1996; Knief and Dunfield 2005). It is known that the affinity for methane can even be in the nM range for growth under atmospheric methane concentrations (Dunfield and Conrad 2000; Baani and Liesack 2008). The fitted half saturation in the lower μM range therefore reflects an adaptation to the low methane concentrations in the mixed layer. The best fit estimate for the CCE of the Monod-type growth model (y) is 0.13 which is in good agreement with the 0.16 estimated from the measurements. Published values for the CCE of MOB vary widely from 0.19 to 0.7 and likely also depend on growth conditions (Leak and Dalton 1986*a*,*b*). The low CCE may partly result from the uncertainty of our biomass estimate but might also reflect the methane-limited conditions, where maintenance energy accounts for a higher proportion of methane oxidation. That

a high respiratory demand decreases the growth efficiency has been shown for various bacteria in lakes (Smith et al. 2009). According to the growth model, the MOB community grew on average at only 26 ± 19% of the maximum growth rate. In addition, the potentially higher metabolic costs of the elevated methane affinity required to thrive at low concentrations might also have reduced the CCE (Knief and Dunfield 2005). The best fit estimate for the maximum specific methane oxidation rate (r_{mox}^{max}) is 1.2 d^{-1} and lies well within the range of specific methane oxidation rates of 0.08–2.3 d^{-1} calculated based on measured methane oxidation rates in Mayr et al. (2020*a*). Combined with the CCE, the maximum specific methane oxidation rate translates to a maximum growth rate of 0.16 d^{-1} or a doubling time of ~4 d. Doubling times reported for pure cultures are typically in the range of a few hours (Joergensen and Degn 1987; Knief and Dunfield 2005; Baani and Liesack 2008), but these values represent growth under optimal or near-optimal conditions. Doubling times in environmental settings are likely to be longer and reported values for freshwater samples are in the range of 2–3 d (Milucka et al. 2015; Oswald et al. 2015, 2016).

Robustness of the microbial methane converter

The velocity of thermocline deepening and the piston velocity of gas exchange with the atmosphere are important factors influencing the efficiency of the microbial methane converter (i.e., the amount of stored methane that is oxidized by MOB before it escapes to the atmosphere). During the autumn overturn in Lake Rotsee, wind and thermal convection played different roles in this respect. Our model calculations show that wind contributed 77 ± 13% to the gas transfer coefficient and that wind was therefore the main driver for the transport of methane from the surface water to the atmosphere. In contrast, wind on average contributed only 5% to the dissipation rate of turbulent kinetic energy at the mixed-layer depth (Fig. 2a, inset). In addition, the Monin–Obukhov length scale, which indicates the depth where wind and convection have equal strength, was smaller than the mixed layer depth (Supplementary Fig. S5) for most of the time. Thermal convection was therefore the dominant driver for the deepening of the thermocline and thus for the supply of stored methane to the mixed layer.

Model simulations of the autumn overturn in Lake Rotsee based on meteorological data from 1990 to 2016 showed that this convective regime dominated throughout those years. The annual variability of stored methane that is oxidized by MOB stayed in a narrow range of 95–98%. Vachon et al. (2019) suggested a correlation between the proportion of stored methane emitted during fall lake overturn and the

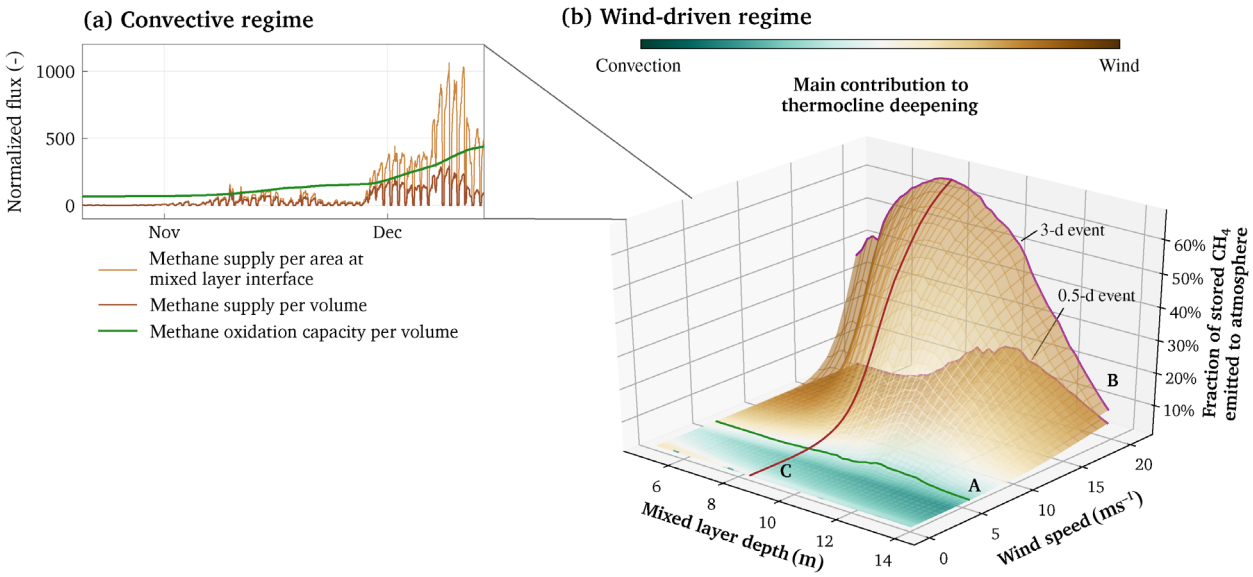

Fig 3. Robustness of the microbial methane converter. (**a**) Typical methane fluxes to the mixed layer for the convective regime (gray lines to panel b indicate the convective regime in the scenario analysis). The methane fluxes were normalized to the minimum nonzero flux and are plotted per cross-section area at the mixed layer interface and per volume of the mixed layer. The flux of stored methane per volume can be compared to the methane oxidation capacity, the maximum rate of methane oxidation of the MOB biomass. (**b**) Scenario analysis for events of elevated wind speeds. The two surfaces represent the fraction of stored methane that is emitted at the end of the overturn period if a 3-d or a 0.5-d wind-event is artificially generated during the overturn period at given wind speeds and mixed layer depths. The two surfaces are colored according to whether wind or convection was the dominant driver for the thermocline deepening. Wind-events started at different mixed-layer depths and consisted of constant wind speeds for the whole duration of the event. Lines A, B, and C highlight specific situations discussed in the text. Line A: Convective regime for wind speeds up to 5.6 m s^{-1}. Line B: Rapid wind-driven mixing for gale-force wind speeds of 20 m s^{-1}. Line C: Fraction of methane emitted to the atmosphere, when a wind-event occurs and the mixed layer has a depth of 8 m.

speed of thermocline deepening. Following the same approach, we obtained an average vertical mixing speed of 0.08 m d^{-1} and a proportion of methane emitted of only 7% confirming a high fraction of oxidized methane.

The fraction of oxidized methane was consistently high. This was a result of the convective mixing regime, with a gradual deepening of the thermocline that kept methane fluxes well below the methane oxidation capacity (Fig. 3a). The average of the daily maximum methane fluxes to the mixed layer never exceeded 27% of the methane oxidation capacity even when deeper water layers with higher methane concentrations were involved. This robustness of the methane converter during the overturn is due to two effects. First, the increasing flux of stored methane to the mixed layer was diluted in an ever-larger volume of the mixed layer. The dilution was three times larger at the end of the overturn compared to the initial situation. Second, the supply of methane increased the MOB biomass and thus methane oxidation capacity.

We used a scenario analysis to explore the extent to which the robustness of the microbial methane converter depends on the velocity of thermocline deepening. Because Lake Rotsee is wind-sheltered, we specifically focused on the effect of higher wind speeds (Fig. 3b). The scenario analysis revealed three important patterns. First, the fraction of stored methane that is emitted to the atmosphere by the end of the overturn period is negligible for wind speeds of up to about 5.6 m s^{-1} (Fig. 3b, line A). For these wind speeds (moderate breeze on the Beaufort scale), convection still dominates the deepening of the thermocline. Second, for a 12-h wind-event, the fraction of emitted methane stayed below 20% even for gale-force wind speeds of up to 20 m s^{-1} (Fig. 3b, line B). To increase this fraction to 60%, 3 d of consecutive wind speeds of 20 m s^{-1} were necessary. Third, the timing of the wind-event matters. The fraction of emitted methane was highest when the wind-event occurred at intermediate mixed-layer depths (Fig. 3b, line C) but was significantly lower if it occurred at the beginning or the end of the overturn period. At the beginning of the overturn, the methane concentrations just below the mixed-layer are low and therefore the potential emissions are low as well. At the end of the overturn period, dilution and the increased MOB biomass keep the emissions low, despite the high methane concentrations.

Conclusions

Our model simulation and scenario analysis suggest that microbial oxidation of stored methane during lake overturn is robust and efficient under a large range of mixing regimes in the studied lake. While our study was conducted on a single wind-sheltered lake, this conclusion is in line with a number of other field observations indicating high proportions of stored methane being oxidized during overturn (Utsumi et al. 1998; Kankaala et al. 2007; Schubert et al. 2012; Encinas Fernández et al. 2014; Vachon et al. 2019). Therefore, global estimates of methane emissions from lakes might indicate upper limits, because they generally assume that all of this methane is emitted to the atmosphere (Bastviken et al. 2004, 2008). Further validation of the robustness and efficiency of the methane oxidation during overturn on a larger set of lakes will be crucial to improve these estimates. We assume that situations similar to Rotsee are present in a significant proportion of lakes globally (Mayr et al. 2020*a*). More rapid thermocline deepening could well limit the ability of the MOB biomass to respond and thus limit the amount of methane oxidized during overturn in some lakes under specific conditions (Vachon et al. 2019). Convective processes are usually the dominant drivers for mixing and stratification because the wind transfer of energy is limited by the reduced fetch, while surface cooling is independent of lake size. Convective forces are therefore increasingly recognized as important drivers for various biogeochemical processes in inland waters (Bouffard and Wüest 2019).

Based on our analysis, we expect that future emissions of stored methane from stratified temperate lakes remain low. Climate change will increasingly strengthen lake stratification and make partial mixing more common (Woolway and Merchant 2019). Even though more extensive anoxic conditions will allow more methane to accumulate, the slower mixing process resulting from strong stratification in turn facilitates its oxidation. In contrast, we expect that the relative importance of ebullition increases, as prolonged hypoxia increases the sediment methane concentration. According to our scenario analysis, elevated emissions of stored methane during autumn overturn are linked to exceptional meteorological events with persistently strong wind for several days or a combination of rapid cooling with strong winds. Estimates of the frequency of extreme wind and cooling events during the autumn overturn might therefore be particularly important to estimate current and future emissions of stored methane, since such events could have larger effects than the average warming trend itself (Woolway et al. 2019).

References

Baani, M., and W. Liesack. 2008. Two isozymes of particulate methane monooxygenase with different methane oxidation kinetics are found in *Methylocystis* sp. strain SC2. Proc. Natl. Acad. Sci. USA **105**: 10203–10208. doi:10.1073/pnas.0702643105

Bastviken, D., J. Cole, M. Pace, and L. Tranvik. 2004. Methane emissions from lakes: Dependence of lake characteristics, two regional assessments, and a global estimate. Global Biogeochem. Cycles **18**: 1–12. doi:10.1029/2004GB002238

Bastviken, D., J. J. Cole, M. L. Pace, and M. C. Van de Bogert. 2008. Fates of methane from different lake habitats: Connecting whole-lake budgets and CH_4 emissions.

J. Geophys. Res. Biogeosci. **113**: 1–13. doi:10.1029/2007JG000608

Batchvarova, E., and S.-E. Gryning. 1991. Applied model for the growth of the daytime mixed layer. Boundary-Layer Meteorol. **56**: 261–274. doi:10.1007/BF00120423

Beaulieu, J. J., T. DelSontro, and J. A. Downing. 2019. Eutrophication will increase methane emissions from lakes and impoundments during the 21st century. Nat. Commun. **10**: 1375. doi:10.1038/s41467-019-09100-5

Bouffard, D., and A. Wüest. 2019. Convection in lakes. Annu. Rev. Fluid Mech. **51**: 189–215. doi:10.1146/annurev-fluid-010518-040506

DelSontro, T., M. J. Kunz, T. Kempter, A. Wüest, B. Wehrli, and D. B. Senn. 2011. Spatial heterogeneity of methane ebullition in a large tropical reservoir. Environ. Sci. Technol. **45**: 9866–9873. doi:10.1021/es2005545

DelSontro, T., J. J. Beaulieu, and J. A. Downing. 2018. Greenhouse gas emissions from lakes and impoundments: Upscaling in the face of global change. Limnol. Oceanogr.: Letters **3**: 64–75. doi:10.1002/lol2.10073

Devlin, S. P., J. Saarenheimo, J. Syväranta, and R. I. Jones. 2015. Top consumer abundance influences lake methane efflux. Nat. Commun. **6**: 8787. doi:10.1038/ncomms9787

Driedonks, A. G. M. 1982. Models and observations of the growth of the atmospheric boundary layer. Boundary-Layer Meteorol. **23**: 283–306. doi:10.1007/BF00121117

Dunfield, P. F., and R. Conrad. 2000. Starvation alters the apparent half-saturation constant for methane in the type II methanotroph *Methylocystis* strain LR1. Appl. Environ. Microbiol. **66**: 4136–4138. doi:10.1128/AEM.66.9.4136-4138.2000

Encinas Fernández, J., F. Peeters, and H. Hofmann. 2014. Importance of the autumn overturn and anoxic conditions in the hypolimnion for the annual methane emissions from a temperate lake. Environ. Sci. Technol. **48**: 7297–7304. doi:10.1021/es4056164

Eugster, W., and P. Plüss. 2010. A fault-tolerant eddy covariance system for measuring CH_4 fluxes. Agric. For. Meteorol. **150**: 841–851. doi:10.1016/j.agrformet.2009.12.008

Hanson, R. S., and T. E. Hanson. 1996. Methanotrophic bacteria. Microbiol. Rev. **60**: 439–471.

Joergensen, L., and H. Degn. 1987. Growth rate and methane affinity of a turbidostatic and oxystatic continuous culture of *Methylococcus capsulatus* (Bath). Biotechnol. Lett. **9**: 71–76. doi:10.1007/BF01043398

Kankaala, P., S. Taipale, H. Nykänen, and R. I. Jones. 2007. Oxidation, efflux, and isotopic fractionation of methane during autumnal turnover in a polyhumic, boreal lake. J. Geophys. Res. Biogeo. **112**: 1–7. doi:10.1029/2006JG000336

Knief, C., and P. F. Dunfield. 2005. Response and adaptation of different methanotrophic bacteria to low methane mixing ratios. Environ. Microbiol. **7**: 1307–1317. doi:10.1111/j.1462-2920.2005.00814.x

Kovárová-Kovar, K., and T. Egli. 1998. Growth kinetics of suspended microbial cells: From single-substrate-controlled growth to mixed-substrate kinetics. Microbiol. Mol. Biol. Rev. **62**: 646–666. doi:10.1128/MMBR.62.3.646-666.1998

Leak, D. J., and H. Dalton. 1986*a*. Growth yields of methanotrophs - 1. Effect of copper on the energetics of methane oxidation. Appl. Microbiol. Biotechnol. **23**: 470–476. doi:10.1007/BF02346062

Leak, D. J., and H. Dalton. 1986*b*. Growth yields of methanotrophs - 2. A theoretical analysis. Appl. Microbiol. Biotechnol. **23**: 477–481.

Liss, P. S., and Slater, P. G. 1974. Flux of gases across the air-sea interface. Nature. **247**: 181–184. doi:10.1038/247181a0

Lorke, A., and F. Peeters. 2006. Toward a unified scaling relation for interfacial fluxes. J. Phys. Oceanogr. **36**: 955–961. doi:10.1175/JPO2903.1

Mayr, M. J., M. Zimmermann, J. Dey, A. Brand, B. Wehrli, and H. Bürgmann. 2020*a*. Growth and rapid succession of methanotrophs effectively limit methane release during lake overturn. Commun. Biol. **3**: 108. doi:10.1038/s42003-020-0838-z

Mayr, M. J., M. Zimmermann, J. Dey, B. Wehrli, and H. Bürgmann. 2020*b*. Lake mixing regime selects apparent methane oxidation kinetics of the methanotroph assemblage. Biogeosciences **17**: 4247–4259. doi:10.5194/bg-17-4247-2020

Milucka, J., M. Kirf, L. Lu, A. Krupke, P. Lam, S. Littmann, M. M. Kuypers, and C. J. Schubert. 2015. Methane oxidation coupled to oxygenic photosynthesis in anoxic waters. ISME J. **9**: 1991–2002. doi:10.1038/ismej.2015.12

Oswald, K., J. Milucka, A. Brand, S. Littmann, B. Wehrli, M. M. M. Kuypers, and C. J. Schubert. 2015. Light-dependent aerobic methane oxidation reduces methane emissions from seasonally stratified lakes. PLoS one **10**: e0132574. doi:10.1371/journal.pone.0132574

Oswald, K., J. Milucka, A. Brand, P. Hach, S. Littmann, B. Wehrli, M. M. M. Kuypers, and C. J. Schubert. 2016. Aerobic gammaproteobacterial methanotrophs mitigate methane emissions from oxic and anoxic lake waters. Limnol. Oceanogr. **61**: S101–S118. doi:10.1002/lno.10312

Posch, T., M. Loferer-Krößbacher, G. Gao, A. Alfreider, J. Pernthaler, and R. Psenner. 2001. Precision of bacterioplankton biomass determination: A comparison of two fluorescent dyes, and of allometric and linear volume-to-carbon conversion factors. Aquat. Microb. Ecol. **25**: 55–63. doi:10.3354/ame025055

Reis, P. C. J., S. D. Thottathil, C. Ruiz-González, and Y. T. Prairie. 2020. Niche separation within aerobic methanotrophic bacteria across lakes and its link to methane oxidation rates. Environ. Microbiol. **22**: 738–751. doi:10.1111/1462-2920.14877

Romanova, N. D., and A. F. Sazhin. 2010. Relationships between the cell volume and the carbon content of bacteria. Oceanology **50**: 522–530. doi:10.1134/S0001437010040089

Schmid, M., I. Ostrovsky, and D. F. McGinnis. 2017. Role of gas ebullition in the methane budget of a deep subtropical lake: What can we learn from process-based modeling? Limnol. Oceanogr. **62**: 2674–2698. doi:10.1002/lno.10598

Schubert, C. J., T. Diem, and W. Eugster. 2012. Methane emissions from a small wind shielded Lake determined by eddy covariance, flux chambers, anchored funnels, and boundary model calculations: A comparison. Environ. Sci. Technol. **46**: 4515–4522. doi:10.1021/es203465x

Smith, E. M., Y. T. Prairie, and S. Carolina. 2009. Bacterial metabolism and growth efficiency in lakes: The importance of availability phosphorus. Limnology **49**: 137–147.

Sollberger, S., B. Wehrli, C. J. Schubert, T. DelSontro, and W. Eugster. 2017. Minor methane emissions from an Alpine hydropower reservoir based on monitoring of diel and seasonal variability. Environ Sci Process Impacts **19**: 1278–1291. doi:10.1039/c7em00232g

Thottathil, S. D., P. C. J. Reis, and Y. T. Prairie. 2019. Methane oxidation kinetics in northern freshwater lakes. Biogeochemistry **143**: 105–116. doi:10.1007/s10533-019-00552-x

Tranvik, L. J., J. J. Cole, and Y. T. Prairie. 2018. The study of carbon in inland waters-from isolated ecosystems to players in the global carbon cycle. Limnol. Oceanogr.: Letters **3**: 41–48. doi:10.1002/lol2.10068

Utsumi, M., Y. Nojiri, T. Nakamura, T. Nozawa, A. Otsuki, N. Takamura, M. Watanabe, and H. Seki. 1998. Dynamics of dissolved methane and methane oxidation in dimictic Lake Nojiri during winter. Limnol. Oceanogr. **43**: 10–17. doi:10.4319/lo.1998.43.1.0010

Vachon, D., T. Langenegger, D. Donis, and D. F. McGinnis. 2019. Influence of water column stratification and mixing patterns on the fate of methane produced in deep sediments of a small eutrophic lake. Limnol. Oceanogr. **64**: 2114–2128. doi:10.1002/lno.11172

Woolway, R. I., and C. J. Merchant. 2019. Worldwide alteration of lake mixing regimes in response to climate change. Nat. Geosci. **12**: 271–276. doi:10.1038/s41561-019-0322-x

Woolway, R. I., G. A. Weyhenmeyer, M. Schmid, M. T. Dokulil, E. de Eyto, S. C. Maberly, L. May, and C. J. Merchant. 2019. Substantial increase in minimum lake surface temperatures under climate change. Clim. Change **155**: 81–94. doi:10.1007/s10584-019-02465-y

Acknowledgments

This research was supported by SNF (grant CR23I3_156759) and ETH Zurich (scientific equipment grants 0-43350-07, 0-23138-09, and 0-43683-11). We thank Karin Beck, Michael Plüss, Michael Schurter, and Christian Dinkel for the technical support during the field campaigns and Jason Dey for CARD-FISH and image analysis.

Submitted 19 December 2019
Revised 20 May 2021
Accepted 25 May 2021